# Effect of $C_{60}$ giant resonance on the photoabsorption of encaged atoms

Zhifan Chen and Alfred Z. Msezane
*Department of Physics and CTSPS, Clark Atlanta University, Atlanta, Georgia 30314, USA*
(Received 31 August 2012; published 11 December 2012)

The absolute differential oscillator strengths (DOSs) for the photoabsorption of the Ne, Ar, and Xe atoms encapsulated in the $C_{60}$ have been evaluated using the time-dependent density-functional theory, which solves the quantum Liouvillian equation with the Lanczos chain method. The calculations are performed in the energy regions both inside and outside the $C_{60}$ giant resonance. The photoabsorption spectra of the atoms encaged in the $C_{60}$ demonstrate strong oscillations inside the energy range of the $C_{60}$ giant resonance. This type of oscillation cannot be explained by the confinement resonance, but is due to the energy transfer from the $C_{60}$ valence electrons to the photoelectron through the intershell coupling.

DOI: 10.1103/PhysRevA.86.063405 PACS number(s): 33.80.Eh, 36.40.−c

## I. INTRODUCTION

Recently a method to evaluate the absolute differential oscillator strengths (DOSs) for the photoabsorption of atoms encapsulated inside a fullerene has been developed [1,2]. This method takes three steps to calculate the photoabsorption spectra of the fullerene and the endohedral fullerene separately. First, the structures of the fullerene and endohedral fullerene are optimized [3]. Second, the ground state eigenvalues and eigenvectors are created by solving the Kohn-Sham equation self-consistently using a supercell [4] and a plane wave approach [5]. Third, the linear response of the system to the perturbation by an external electric field is described by the quantum Liouvillian equation [6]. The photoabsorption spectra are evaluated using the time-dependent density-functional theory (TDDFT) with the Liouville-Lanczos approach [7,8]. Finally, the absolute DOSs for the photoabsorption of an atom encapsulated inside a fullerene can be calculated approximately by subtracting the DOSs of the fullerene from the corresponding DOSs of the endohedral fullerene at the same photon energy.

This method has been successfully used to study the photoabsorption spectra of the $Xe@C_{60}$ [1] and $Sc_3N@C_{80}$ [2] molecules. These examples demonstrate the great advantage of the method. The method can be used to study the atoms located at the center of the fullerene [1] and the off-center positions as well [2]. It also allows us to evaluate the spectrum in a broad energy region.

In the photoionization studies of endohedral fullerenes the most interesting problem is probably the Xe $4d$ giant resonance of the $Xe@C_{60}$ molecule [9–14]. The theoretical calculations that used model potentials [10,13] and the TDDFT with the jellium approximation [12] ignored the effect of the $C_{60}$ giant resonance because, fortunately the Xe $4d$ giant resonance is found at the energy region far from the $C_{60}$ resonance. Amusia and Baltenkov [15] and Madjet *et al.* [16] have studied the $C_{60}$ resonance effects on the photoionization cross sections of the Xe $5s$ and Ar $3p$ electrons encaged in the $C_{60}$. However, the photoabsorption spectra of the Ar and Xe atoms encapsulated in the $C_{60}$ is still unknown. In this paper we have evaluated the absolute DOSs for the photoabsorption of the Ne, Ar, and Xe atoms encapsulated in the $C_{60}$ in the regions both inside and outside the $C_{60}$ giant resonance. The results demonstrate a strong oscillation and a significant increase of the DOSs in the $C_{60}$ resonance region for all these atoms.

## II. METHOD

As stated in the Introduction the method of calculation used here takes three steps to evaluate the photoabsorption spectra of the fullerene and endohedral fullerene. In the first step we utilize the DMol$_3$ software package [3] to determine the optimized structure of the fullerene. Geometry optimization of the $C_{60}$ was performed using the generalized gradient approximation (GGA) to the density-functional theory (DFT) [4], with the Perdew-Burke-Ernzerhof (PBE) exchange-correlation functional [17] along with all electrons double numerical plus polarization (DNP) basis sets and dispersion correction as implemented in the DMol$_3$ package [3]. The optimization of atomic positions proceeded until the change in energy was less than $5 \times 10^{-4}$ eV and the forces were less than 0.01 eV Å$^{-1}$. Those parameters can also be used for the optimization of the endohedral fullerene. The optimized structure was then introduced into a supercell of 18 Å. The Kohn-Sham equation was solved self-consistently to create the ground state eigenvalues and eigenvectors for the total of 240 electrons and 120 states using the plane wave approach [5]. An ultrasoft pseudopotential using Rappe-Rabe-Kaxiras-Joannopoulos (RRKJ) pseudization algorithms [18], which replace atomic orbitals in the core region with smooth nodeless pseudo-orbitals, has been employed in the calculation. The kinetic energy cutoff of 408 eV for the wave function and 2448 eV for the densities and potentials were employed in a standard ground state DFT calculation [5]. The linear response of the ground state to an external perturbation by an electric field was described by the quantum Liouvillian equation [6,7](atomic units are used throughout, unless stated otherwise):

$$i\frac{d\rho}{dt} = [H_{KS}(t), \rho(t)], \tag{1}$$

where $H_{KS}(t)$ is the time dependent Kohn-Sham (KS) Hamiltonian and $\rho(t)$ is the one-electron KS density matrix. The KS Hamiltonian can be written as

$$H_{KS}(t) = -\tfrac{1}{2}\nabla^2 + v_{ext}(\mathbf{r},t) + v_{Hxc}(\mathbf{r},t), \tag{2}$$

where $v_{ext}(\mathbf{r},t)$ is the external potential and $v_{Hxc}(\mathbf{r},t)$ is the time dependent Hartree potential plus the exchange-correlation potential.

 

Linearization of Eq. (1) with respect to the external perturbation leads to

$$i\frac{d\rho'}{dt} = \left[H_{KS}^{GS}, \rho'(t)\right] + [v'_{Hxc}(t), \rho_0] + [v'_{ext}(t), \rho_0], \quad (3)$$

where $H_{KS}^{GS}$ is the time-independent ground-state Hamiltonian, $v'_{ext}(t)$ is the perturbing external potential, $v'_{Hxc}(t)$ is a linear variation of the Hartree plus exchange-correlation potentials induced by $\rho'(t)$. $\rho'(t) = \rho(t) - \rho_0$. The linearized Liouvillian equation is given by

$$i\frac{d\rho'(t)}{dt} = \mathcal{L}\rho' + [v'_{ext}(t), \rho_0]. \quad (4)$$

The action of the Liouvillian superoperator $\mathcal{L}$ on $\rho'$ is given by

$$\mathcal{L}\rho' = \left[H_{KS}^{GS}, \rho'\right] + [v'_{Hxc}[\rho'](t), \rho_0]. \quad (5)$$

Fourier analyzing Eq. (4) we have

$$(w - \mathcal{L})\rho'(w) = [v'_{ext}(w), \rho_0]. \quad (6)$$

If $v'_{ext}(\mathbf{r}, w) = -\mathbf{E}(w)\cdot\mathbf{r}$, the response of the dipole to an external electric field $\mathbf{E}(w)$ is given by

$$d_i(w) = \sum \alpha_{ij} E_j(w). \quad (7)$$

The dynamical polarizability, $\alpha_{ij}(\omega)$ is defined by

$$\alpha_{ij}(\omega) = - < r_i | \frac{[r_j, \rho_0]}{(w - \mathcal{L})} > . \quad (8)$$

Equation (8) indicates that the dynamical polarizability can be expressed as an appropriate off-diagonal matrix element of the resolvent of the non-Hermitian Liouvillian superoperator between two orthogonal vectors [6]. These matrix elements are calculated using the Lanczos algorithm [7,8]. Finally the absolute DOSs of the $C_{60}$ are obtained from

$$S(\omega) = \frac{4\omega}{3\pi} \sum \mathrm{Im}\, \alpha_{jj}. \quad (9)$$

After the $C_{60}$ calculation a Xe (Ne or Ar) atom was introduced into the center of the $C_{60}$. It should be noted that when the $C_{60}$ carbon orbitals are mixed with the orbitals of the encaged atom the initial energy levels of the $C_{60}$, Ne, Ar, Xe, etc., will be changed under the hybridization effect. The DOSs of the Xe@$C_{60}$ was evaluated using the same procedure as described above. Finally the DOSs of Xe atom encapsulated in the $C_{60}$ were obtained in an approximated way by subtracting the DOSs of the $C_{60}$ from the corresponding DOSs of the Xe@$C_{60}$ molecule.

## III. RESULTS

Figure 1 presents the spectra of a Xe atom encapsulated inside the $C_{60}$ in the energy range of the Xe 4*d* giant resonance. A solid curve and a dashed curve represent, respectively, the results of the TDDFT [1] and using our $C_{60}$ model potential [13]. Both the TDDFT and model potential results confirm the three main peaks observed in the experiment [14] if the spectra are reduced by a factor of 8 or 10 as discussed in Refs. [1,13].

The photoabsorption spectrum of the Xe atom encapsulated in the $C_{60}$ in the energy region of $C_{60}$ giant resonance can be evaluated using the same method as mentioned above. It is well known that there are two giant resonances in the $C_{60}$ photoionization spectrum [19–21], which correspond to a collective oscillation of the 240 delocalized valence electrons relative to the ionic cage of the $C_{60}$ fullerene. These delocalized electrons are distributed over the surface but confined in a thickness of a single carbon atom in the radial direction. The valence electrons can move coherently in photoexcitation. The strong peak around 6.3 eV [19] is interpreted as collective excitations of the $\pi$ electrons; the giant resonance between 15–25 eV, peaked at 22 eV, belongs to the $\sigma$ electrons [20,21]. In addition to these there are two broad structures around, respectively, 29 and 32 eV, which are caused by shape resonance [21]. The whole $C_{60}$ spectrum can be found in Ref. [1].

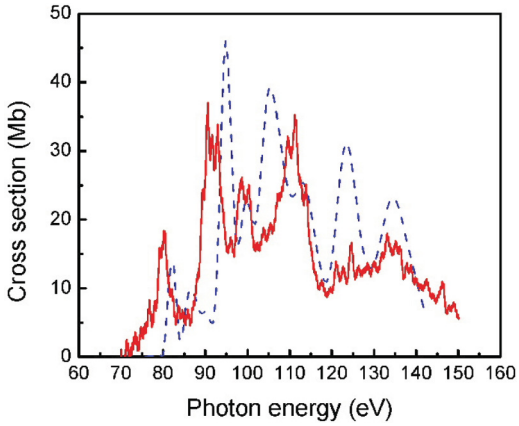


FIG. 1. (Color online) Photoabsorption spectra of a Xe atom encapsulated inside $C_{60}$ in the energy range of the Xe 4*d* giant resonance. Solid and dashed curves represent, respectively, the results of our TDDFT [1] and the $C_{60}$ model potential calculation [13].

Solid and dashed curves in Fig. 2 are, respectively, the absolute DOSs for the photoabsorption of the encapsulated and free Xe atom calculated by TDDFT method. In the energy range 65–140 eV, the solid curve is the same as that in Fig. 1. Within the $C_{60}$ giant resonance region the spectrum of the Xe

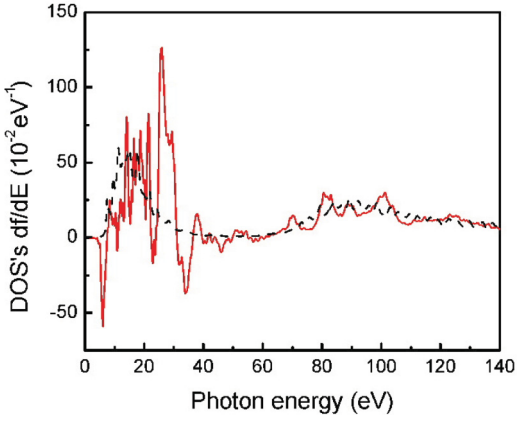


FIG. 2. (Color online) Absolute DOSs for the photoabsorption of the Xe atom. Solid and dashed curves represent, respectively, the TDDFT results of the encapsulated and free Xe atoms.

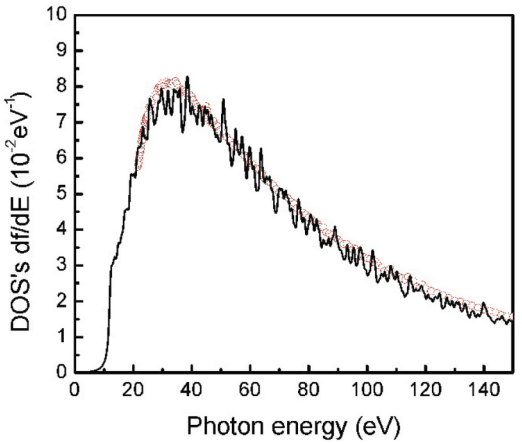


FIG. 3. (Color online) Absolute DOSs for the photoabsorption of a free Neon atom. Solid curve and open circles represent, respectively, our TDDFT calculation and the experimental data [23].

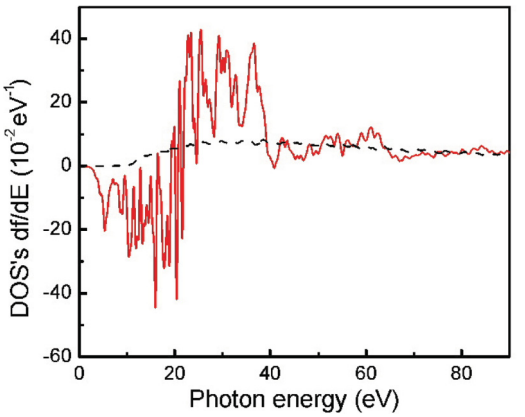


FIG. 5. (Color online) Solid and dashed curves are, respectively, the calculated absolute DOSs for the photoabsorption of the encapsulated and free Ne atoms.

atom encapsulated in the $C_{60}$ shows strong oscillation. It is noted that the absolute DOSs for the atom encapsulated in the $C_{60}$ was obtained by subtracting the DOSs of the $C_{60}$ from the corresponding results of the $Xe@C_{60}$ molecule. Therefore if the DOSs of the $C_{60}$ fullerene are larger than the DOSs of the $Xe@C_{60}$ molecule the curve has negative values. This means that the Xe atom disturbed the $C_{60}$ resonance and reduced the DOSs of the $C_{60}$. Figure 2 indicates that the negative value usually happens in the low energy range. If the photon energy cannot ionize the Xe $5p$ electron the $C_{60}$ valence electrons hardly transfer their resonance energy to the Xe electrons through intershell coupling. Otherwise the energy transfer from $C_{60}$ valence electrons to the photoelectron is strong. Because of this, the peak at 25 eV may be related to the Xe $5s$ ionization (see Fig. 2). The ionization threshold for the $5s$ of a free Xe is 25.4 eV.

Strong oscillations as in Fig. 2 can also be found in the spectra of the Ne and Ar atoms encapsulated in the $C_{60}$. In the following, we first evaluate the DOSs for the photoabsorption of the free Ne and Ar atoms. The ultrasoft pseudopotentials for these atoms have been created using the PBE [17] exchange-correlation functional and including the relativistic effect and nonlinear core corrections [22]. The valence electrons for Ne and Ar are, respectively, $2s$, $2p$ and $3s$, $3p$. Solid curves in Figs. 3 and 4 are, respectively, the calculated absolute DOSs for the free Ne and Ar atoms. The open circles in Figs. 3 and 4 represent the corresponding experimental data [23,24]. The measurements used the low-resolution dipole spectrometer. The data started from the first ionization potentials, 21.6 eV of the Ne $2p$ state and 16.0 eV of the Ar $3p$ state. The present TDDFT calculations are in good agreement with the experimental results reported by Refs. [23,24].

The solid curves in both Figs. 3 and 4 rise rapidly initially. The experimental spectra of Ne and Ar reach their maxima, respectively, at the 31.5 and 21.6 eV. After reaching its maximum the Ar curve drops quickly to approach the Cooper minimum around 47 eV. The $3s$ ionization threshold of a free Ar atom is about 34.7 eV. At this energy a small peak is found in the theoretical curve.

The curves in Figs. 3 and 4 demonstrate that our ultrasoft pseudopotentials describe the photoabsorption processes of the Ne and Ar atoms very well. The photoabsorption spectra

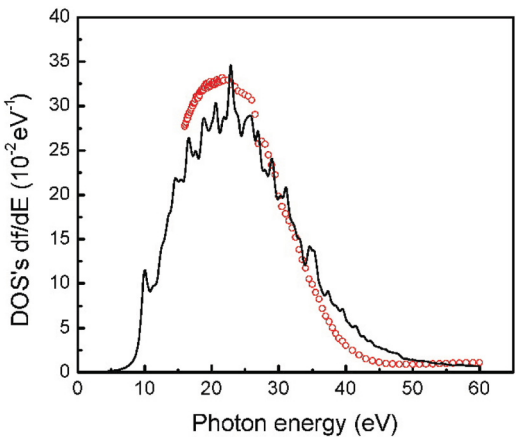


FIG. 4. (Color online) The symbols have the same meaning as in Fig. 3, except that the curve and open circles represent the free Ar atom.

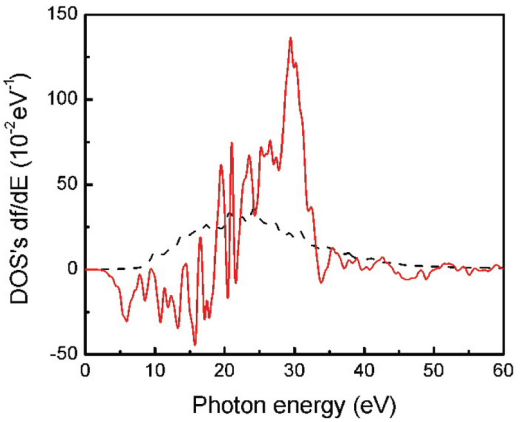


FIG. 6. (Color online) The symbols have the same meaning as in Fig. 5, except that the curves represent the data for the Ar atom.

of the endohedral fullerenes, Ne@$C_{60}$ and Ar@$C_{60}$, have also been calculated using the same TDDFT method. The DOSs of the Ne and Ar atoms encapsulated in the $C_{60}$ are obtained by subtracting the DOSs of the $C_{60}$ from the corresponding DOSs of the endohedral fullerenes.

Dashed and solid curves in Figs. 5 and 6 represent the DOSs for the photoabsorption of the free and encaged Ne and Ar atoms, respectively. The solid curves in Figs. 5 and 6 demonstrate the strong oscillations in the region of the $C_{60}$ giant resonance. The solid curve in Fig. 5 can be divided roughly into two parts, a positive part and a negative part. When the photon energy is larger than the first ionization potential of the Ne atom the DOSs show positive values. This implies that the $C_{60}$ valence electrons transfer resonance energy to the photoelectron through intershell coupling. Otherwise the resonance of the $C_{60}$ is perturbed and the DOSs are reduced by the Ne atom.

Figure 6 shows that when the photon energy is large the DOSs are positive; otherwise the DOSs of the $C_{60}$ are reduced by the Ar atom. This causes negative DOSs of the Ar atom encaged in the $C_{60}$.

The solid curves in Figs. 2, 5, and 6 demonstrate that the DOSs of the atoms encaged in the $C_{60}$ are positive only when the photon energies are large. This indicates that strong energy transfer can occur only between the $C_{60}$ valence electrons and the photoelectron.

## IV. CONCLUSION

In conclusion, the absolute DOSs for the photoabsorption of the Ne, Ar, and Xe atoms encapsulated in the $C_{60}$ have been calculated in the energy regions both inside and outside the $C_{60}$ giant resonance. Within the $C_{60}$ giant resonance the spectra of the Ne, Ar, and Xe atoms encaged in the $C_{60}$ demonstrate strong oscillation with significant increase of the DOSs. This large enhancement of the DOSs cannot be explained by confinement resonance but is due to the energy transfer from the $C_{60}$ valence electrons to the photoelectron through the intershell coupling. The energy transfer occurs only when the photon energy is large enough to ionize the atom encapsulated in the $C_{60}$. To study the confinement resonance it is recommended to avoid the $C_{60}$ resonance region by selecting the photon energy larger than 40 eV.

## ACKNOWLEDGMENTS

This work was supported by the U.S. DOE, Division of Chemical Sciences, Geosciences, and Biosciences, Office of Basic Energy Sciences, Office of Energy Research, AFOSR, and Army Research Office (Grant No. W911NF-11-1-0194). Calculations used the Kraken System (account No. TG-DMR120078) of the National Institute for Computational Science, The University of Tennessee.

[1] Zhifan Chen and A. Z. Msezane, Eur. Phys. J. D **66**, 184 (2012).
[2] Zhifan Chen and A. Z. Msezane, J. Phys. B: At. Mol. Opt. Phys. **45**, 235205 (2012).
[3] DMol$_3$ (Accelrys Software Inc., San Diego, CA, 2010).
[4] R. M. Martin, *Electronic Structure: Basic Theory and Practical Methods* (Cambridge University Press, Cambridge, 2004).
[5] P. Giannozzi *et al.*, J. Phys.: Condens. Matter **21**, 395502 (2009).
[6] B. Walker, A. M. Saitta, R. Gebauer, and S. Baroni, Phys. Rev. Lett. **96**, 113001 (2006).
[7] D. Rocca, R. Gebauer, Y. Saad, and S. Baroni, J. Chem. Phys. **128**, 154105 (2008).
[8] S. Baroni *et al.*, J. Phys.: Condens. Matter **22**, 074204 (2010).
[9] M. J. Puska and R. M. Nieminen, Phys. Rev. A **47**, 1181 (1993).
[10] M. Ya. Amusia, A. S. Baltenkov, L. V. Chernysheva, Z. Felfli, and A. Z. Msezane, J. Phys. B **38**, L169 (2005).
[11] M. Ya. Amusia, L. V. Chernysheva, and V. K. Dolmatov, Phys. Rev. A **84**, 063201 (2011).
[12] M. E. Madjet, T. Renger, D. E. Hopper, M. A. McCune, H. S. Chakraborty, Jan-M. Rost, and S. T. Manson, Phys. Rev. A **81**, 013202 (2010).
[13] Zhifan Chen and A. Z. Msezane, Eur. Phys. J. D **65**, 353 (2011).
[14] A. L. D. Kilcoyne *et al.*, Phys. Rev. Lett. **105**, 213001 (2010).
[15] M. Ya. Amusia and A. S. Baltenkov, Phys. Rev. A **73**, 062723 (2006).
[16] M. E. Madjet, H. S. Chakraborty, and S. T. Manson, Phys. Rev. Lett. **99**, 243003 (2007).
[17] J. P. Perdew, K. Burke, and M. Ernzerhof, Phys. Rev. Lett. **78**, 1396 (1997).
[18] A. M. Rappe, K. M. Rabe, E. Kaxiras, and J. D. Joannopoulos, Phys. Rev. B **41**, 1227 (1990).
[19] E. Westin *et al.*, J. Phys. B **29**, 5087 (1996).
[20] J. Berkowitz, J. Chem. Phys. **111**, 1446 (1999).
[21] J. Kou *et al.*, Chem. Phys. Lett. **374**, 1 (2003).
[22] D. Vanderbilt, Phys. Rev. B **41**, 7892 (1990).
[23] W. F. Chan, G. Cooper, X. Guo, and C. E. Brion, Phys. Rev. A **45**, 1420 (1992).
[24] W. F. Chan, G. Cooper, X. Guo, G. R. Burton, and C. E. Brion, Phys. Rev. A **46**, 149 (1992).